ELSEVIER

Void bounds for fluid transport in sea ice

K.M. Golden [a,*], A.L. Heaton [a], H. Eicken [b], V.I. Lytle [c]

[a] *Department of Mathematics, University of Utah, 155 S 1400 E RM 233, Salt Lake City, UT 84112-0090, USA*
[b] *Geophysical Institute, P.O. Box 757320, 903 Koyukuk Drive, University of Alaska, Fairbanks, AK 99775-7320, USA*
[c] *CliC International Project Office, Norwegian Polar Institute, Polarmiljsenteret, NO-9296 Tromsø, Norway*

Abstract

Arctic and Antarctic sea ice plays a critical role in the global ocean–climate system, as well as in polar biology. Sea ice is a porous composite of pure ice with brine, air and salt inclusions whose microstructure varies significantly with temperature. The fluid transport properties of sea ice control a broad range of geophysical and biological processes. Yet little is known, for example, about bulk flow of brine or diffusive transport of dissolved substances such as nutrients or pollutants through the porous microstructure, particularly from a theoretical standpoint. Here we give rigorous, mathematical formulations of the two key problems of fluid dynamics in sea ice: estimating the effective fluid permeability tensor $\mathbf{k}(\phi)$ and its dependence on brine porosity ϕ, and estimating the trapping constant γ or mean survival time τ for a diffusion process in the pore microstructure which can react with the boundary. We bring together and review a variety of results which lay the foundation for studying fluid transport processes in sea ice from a mathematical perspective, and focus on rigorous bounds on $\mathbf{k}$ and γ. Void bounds evaluated by Torquato and Pham [Torquato, S., Pham, D.C., 2004. Optimal bounds on the trapping constant and permeability of porous media. Phys. Rev. Lett. 92, 255505:1–4] for classical coated cylinder geometries yield *pipe bounds* for the permeability k of sea ice in the vertical direction. By incorporating information about average brine inclusion sizes, the void bounds provide a useful benchmark that captures laboratory data taken on $k(\phi)$.
© 2005 Elsevier Ltd. All rights reserved.

Keywords: Sea ice; Porous media; Permeability; Trapping; Bounds

1. Introduction

As the thin boundary layer separating the ocean and atmosphere in the polar regions, sea ice plays a key role in polar oceanography and meteorology, and is a sensitive indicator of global climatic change (Untersteiner (Ed.), 1986; Jeffries (Ed.), 1998; Untersteiner, 1990; Kattenberg et al., 1996; Serreze et al., 2000; Sturm et al., October 2003; Perovich et al., 1999). Moreover, polar sea ice serves as a critical habitat for robust algal and bacterial communities which form the base of the rich food web of the sea ice environment (Thomas and Dieckmann (Eds.), 2003; Fritsen et al., 1994; Lizotte and Arrigo (Eds.), 1998; Eicken, 1992). As a material, sea ice is

---

* Corresponding author.
E-mail addresses: golden@math.utah.edu (K.M. Golden), heaton@chem.utah.edu (A.L. Heaton), hajo.eicken@gi.alaska.edu (H. Eicken), victoria.lytle@npolar.no (V.I. Lytle).

a porous composite of pure ice with brine, air and salt inclusions (Weeks and Ackley, 1986; Eicken, 2003), whose microstructure and transport properties change significantly with temperature. Fluid transport in sea ice plays an important role in heat transfer between the ocean and atmosphere (Lytle and Ackley, 1996; Trodahl et al., 2000), ice production through the flooding and subsequent refreezing of ice surfaces (Maksym and Jeffries, 2001; Ackley et al., 1995), and in the input of brine and fresh water into the upper ocean from freezing, melting, and drainage processes (Weeks and Ackley, 1986; Thomas and Dieckmann (Eds.), 2003; Carmack, 1986), as well as in remote sensing (Hosseinmostafa et al., 1995; Lytle and Golden, 1995; Golden et al., 1998c,b). Brine transport substantially controls the replenishment of nutrients for sea ice micro-organisms (Fritsen et al., 1994; Lizotte and Arrigo (Eds.), 1998), and brine itself is the avenue through which bacteria forage for their sustinence. Recently there has even been speculation about the possibility of primitive life forms existing on sea ice-covered extraterrestrial bodies such as Europa (Thomas and Dieckmann, 2002). One reason that sea ice on earth has attracted recent attention is that it can teach us about how organisms cope with cold, extreme environments. The fluid transport properties of sea ice and its complex microstructure play a key role in how micro-organisms living in earth's sea ice survive and thrive in a very harsh environment.

Despite the pervasiveness of geophysical and biological problems where a quantitative, theoretical understanding of the vertical fluid permeability k for sea ice is needed, little is known. There are a few observations of k (Ono and Kasai, 1985; Saito and Ono, 1978), yet measurements which are carefully correlated with information about the microstructure have only recently been made by Freitag (1999). From a theoretical standpoint even less is known. It has long been observed (Cox and Weeks, 1975; Weeks and Ackley, 1986) that macroscopic effects of fluid transport through sea ice, such as changes in salinity due to brine drainage, become significantly more noticeable for brine volume fractions ϕ above a threshold value ϕ_c of roughly 5% or larger. For a typical sea ice salinity of 5 parts per thousand (ppt), this critical porosity ϕ_c corresponds, via a formula relating brine volume to salinity and temperature (Weeks and Ackley, 1986; Eicken, 2003), to a critical temperature $T_c \approx -5\,^\circ\text{C}$. This *rule of fives* is exhibited by classic, large-

grained columnar sea ice, and noticeably higher values of ϕ_c are seen in fine grained frazil ice with more random crystalline configurations. Still, the critical porosities ϕ_c seen in sea ice are much lower than the 20–60% range for percolation thresholds exhibited by standard lattice models in two and three dimensions (Stauffer and Aharony, 1992), and by random arrays of ellipsoids (DeBondt et al., 1992) in the continuum, a commonly used model for the brine inclusions. The brine inclusions in sea ice, however, are situated primarily on the boundaries between individual ice lamellae, which are similar to plates.

It was observed by Golden et al. (1998a) that the microstructure of sea ice can be approximated by that of compressed powders (Kusy and Turner, 1971) of large polymer spheres and much smaller metal or carbon black spheres, used in radar absorbing technology (Priou (Ed.), 1992) and other engineering applications. Continuum percolation models were developed to predict the critical volume fraction of the smaller metal spheres required for percolation (Kusy and Turner, 1971; Malliaris and Turner, 1971; Kusy, 1977; Janzen, 1980, 1975). Compressed powder microstructures facilitated achievement of desired conductivity properties with very low critical volume fractions, while maintaining key properties of the host polymer. The compressed powder model was adapted (Golden et al., 1998a) to explain the rule of fives in sea ice, and a range of Antarctic data on ice production, thermal transport, and biological processes. It was also pointed out that percolation theory explains the general trend of the one limited data set on fluid permeability available then (Ono and Kasai, 1985) which was suitable for comparison, although no theoretical predictions were made.

Here, we find a deceptively simple theoretical result for the behavior of the vertical fluid permeability of sea ice and its dependence upon the microstructure, in the form of a rigorous upper bound. The result can be understood by asking how inclusions of a given volume fraction should be arranged in order to maximize the permeability in the vertical direction. Intuitively, the best arrangement is in vertical pipes, so that no inclusion is wasted in the process of fluid transport, and there are no impediments to flow. Similar findings for laminate geometries which realize the arithmetic mean bounds on effective electrical or thermal conductivity, or effective dielectric constant or magnetic permeability of two phase composites have been known since the

early 1900s. However, bounds such as these for fluid permeability, which involve an inclusion length scale not present in similar electrical, magnetic, or thermal transport problems, were only recently proven by Torquato and Pham (2004). We incorporate known microstructural information about brine inclusions in sea ice (Perovich and Gow, 1996; Bock and Eicken, 2005) into these *void bounds* to obtain the first rigorous, theoretical estimates of fluid permeability in sea ice.

Given the central role that fluid transport plays in the geophysics and biology of sea ice, and the absence of works in this direction, here we give a mathematical formulation of the permeability problem, and the related problem of diffusion in the pore microstructure. We bring together and review methods, results, and theoretical ideas which play a role in yielding the pipe bounds, and which lay the groundwork for further investigations. In particular, our findings here provide a basis for comparison with the results of a two-dimensional network model for bulk fluid transport through sea ice (Zhu et al., submitted for publication). In this random pipe network the radii of the pipes are chosen from distributions describing measured brine inclusion cross-sectional areas (Perovich and Gow, 1996; Bock and Eicken, 2005).

Unlike problems of effective electrical conductivity or permittivity in the quasistatic limit, in fluid transport there is a length scale involved that changes the nature of the results. The electrical conductance g_e of a cylinder of unit length and radius r is $g_e = \pi r^2 \sigma$, where σ is the conductivity of the material. On the other hand, the corresponding fluid conductance g_f of a pipe of unit length and inner radius r is $g_f = \pi r^4 / 8\mu$, where μ is the viscosity of the fluid. Whereas the electrical conductivity is a property of the material, and does not depend on the size of the conductor, the corresponding *fluid* conductivity $r^2 / 8\eta$, depends upon the cross-sectional area of the pipe, as well as the viscosity of the fluid. Consequently, for fluid flow, the permeability of a parallel array of many pipes of small radius is less than that of a few pipes of larger radius occupying the same volume fraction. Another manifestation of the difference between fluid and electrical problems are the different scalings required to obtain appropriate infinite volume limits for the permeability and the electrical conductivity in lattice models (Chayes and Chayes, 1986; Golden, 1997).

By considering here a simplified, parallel pipe model of the brine microstructure of sea ice, we obtain an upper bound on its vertical fluid permeability k, given information about the porosity ϕ and pore length scale. The bound compares well with laboratory data on k considered here, as well as with field data presented in Heaton et al. (2005), where a different form of the bound is considered. We also consider some data taken on the radii and density of large pipes observed in the Antarctic. These data yield an interesting constant, found by Heaton et al. (2005) from other theoretical and microstructural considerations, which appears to provide a general upper bound for the full range of all known data on sea ice fluid permeability.

As discussed above, our pipe bound is a special case of a set of rigorous bounds on the fluid permeability of a porous medium, called *void bounds* (Torquato, 2002). Upper bounds on the fluid permeability of a statistically isotropic porous medium were first proposed by Prager (1961), and a coefficient in these bounds was corrected by Berryman and Milton (1985). The bounds depend on the two-point correlation function of the pore space, and novel variational formulations which yield these and other bounds were found by Rubinstein and Torquato (1989) and Torquato (2002). The void bounds were evaluated explicitly by Torquato and Pham (2004) for coated sphere and coated cylinder geometries. In some cases these bounds are optimal. The simple array of vertical pipes we have used to model the brine microstructure in sea ice is such an optimal geometry. The pipes provide a rigorous upper bound for the permeability of an appropriate class of microstructures sharing the same porosity and characteristic pore length scale. It is interesting to note that the variational principles developed and used to derive bounds on the permeability (Rubinstein and Torquato, 1989; Torquato, 2002; Torquato and Pham, 2004) apply similarly to bounding the *trapping constant* γ or the *mean survival time* $\tau \sim \gamma^{-1}$ for a porous medium. If a reactant diffusing in the pore space can be absorbed by traps on the boundaries, then there is an average time which the reactant can be expected to survive, which is closely related to the permeability. Many processes in porous media depend upon such considerations, and in sea ice they are of particular interest. In nuclear magnetic resonance imaging, the NMR survival time is equivalent to τ, and this type of imaging is particularly promising for sea ice (Eicken et al., 2000). Moreover, bacterial foraging (Vetter et al., 1998) in a porous medium involves diffusion and reaction processes where

knowledge of the trapping constant and survival time may well provide useful biological information.

We remark that in reviewing the porous media literature, we found the seminal and extensive contributions of Torquato and coauthors (Torquato, 2002; Torquato and Pham, 2004; Rubinstein and Torquato, 1989; Torquato, 1990; Torquato and Avellaneda, 1991) to be particularly important and illuminating in addressing the problem of fluid transport through sea ice. Consequently in what follows, these works of Torquato in different contexts dominate our formulation and discussions, and play a key role in the results for sea ice.

2. Homogenization for permeability and trapping in porous random media

2.1. Fluid flow in a porous medium

We consider low Reynolds number flow of a fluid with viscosity μ through a porous random medium, occupying a region $\Omega \subset \mathbb{R}^3$. Brine of viscosity μ occupies the brine pore space $\Omega_b \subset \Omega$, having a relative volume fraction ϕ. The solid ice phase occupies the ice grain space $\Omega_i \subset \Omega$, having a relative volume fraction $1 - \phi$. Let (Θ, P) be a probability space characterizing the porous medium, where Θ is the set of realizations of the random medium and P is a probability measure on Θ. For any realization $\omega \in \Theta$, let $\mathcal{I}(x, \omega)$ be the indicator function of the brine pore space $\Omega_b(\omega)$,

$$\mathcal{I}(x, \omega) = \begin{cases} 1, & x \in \Omega_b(\omega), \\ 0, & x \in \Omega_i(\omega). \end{cases} \tag{1}$$

We first assume that $\mathcal{I}(x, \omega)$ is a stationary random field such that P has translation invariant statistics. Then the medium is statistically homogeneous, and satisfies an *ergodic hypothesis*, where ensemble averaging over realizations $\omega \in \Theta$ is equivalent to an infinite volume limit $|\Omega| \to \infty$ of an integral average over $\Omega \subset \mathbb{R}^3$, denoted by $\langle \cdot \rangle$ (Torquato, 2002). This and related limits have been shown to exist and to be equal to the ensemble average in some situations, thus establishing the ergodic hypothesis, which is discussed below.

We are interested in sea ice as a porous medium for a given temperature T and salinity S, which determine the brine volume fraction ϕ (Weeks and Ackley, 1986; Eicken, 2003). Within a given depth range in an ice sheet, the microstructural characteristics can be quite uniform over many meters horizontally. In such layers the ergodic hypothesis is

satisfied. However, we are also interested in how the properties of the ice vary with depth, where variations in temperature and salinity, as well as possibly ice type and age, affect brine microstructural features and transport properties. Typically, as with many other porous media (Torquato, 2002), not just sea ice, there is a microscopic length scale ℓ associated with the medium. For example, the scale over which the two point correlation function obtained from $\mathcal{I}(x)$ varies, is a good measure of this length. It is small compared to a typical macroscopic length scale L, such as a sample size or thickness of a statistically homogeneous layer. Then the parameter $\epsilon = \ell/L$ is small, and one is interested in obtaining the effective fluid transport behavior in the limit as $\epsilon \to 0$. To obtain such information, the method of *two-scale homogenization* or *two-scale convergence* (Rubinstein and Torquato, 1989; Torquato, 2002; Hornung (Ed.), 1997) has been developed in various forms, based on the identification of two scales: a slow scale x and a fast scale $y = x/\epsilon$. The velocity and pressure fields in the brine, $v^\epsilon(x)$ and $p^\epsilon(x)$ with $x \in \Omega_b(\omega)$, are assumed to depend on these two scales x and y. The idea is to *average*, or *homogenize* over the fast microstructural scale, leading to a simpler equation describing the overall behavior of the flow, Darcy's law. Slower variations of average microstructural properties can then be incorporated through dependence of the effective permeability tensor on x, such as with depth in the sea ice.

The velocity and pressure in the brine phase satisfy the Stokes equations,

$$\nabla p^\epsilon = \mu \Delta v^\epsilon, \quad x \in \Omega_b(\omega), \tag{2}$$

$$\nabla \cdot v^\epsilon = 0, \quad x \in \Omega_b(\omega), \tag{3}$$

$$v^\epsilon(x) = 0, \quad x \in \partial \Omega_b(\omega). \tag{4}$$

A force acting on the medium such as gravity can be incorporated into p^ϵ. Eq. (2) is the steady state fluid momentum equation in the zero Reynolds number limit, (3) is the incompressibility condition, and (4) is the no-slip boundary condition on the pore surface. The macroscopic equations can be derived through a two-scale expansion (Keller, 1980; Tartar, 1980; Rubinstein and Torquato, 1989; Allaire, 1992; Allaire, 1997; Torquato, 2002; Sahimi, 1995; Hornung (Ed.), 1997)

$$v^\epsilon(x) = \epsilon^2 v_0(x, y, \omega) + \epsilon^3 v_1(x, y, \omega) + \cdots \tag{5}$$

$$p^\epsilon(x) = p_0(x) + \epsilon p_1(x, y, \omega) + \cdots \tag{6}$$

Note that the leading term in the velocity expansion is $O(\epsilon^2)$, while the leading term in the pressure

expansion is $O(1)$. This physical effect was handled by Allaire (1997, 1992) analytically by scaling the viscosity of the fluid by $O(\epsilon^2)$. Physically, the very small viscosity of order ϵ^2 exactly balances the friction of the fluid from the no-slip boundary condition on the solid boundaries of the pores. Substitution of the two-scale expansion into the Stokes equations yields systems of equations involving both x and y derivatives. Analysis of the leading order system is facilitated by consideration of a second-order tensor "velocity" field $\mathbf{w}(y,\omega)$ and a vector "pressure" field $\pi(y,\omega)$ (Torquato, 2002), both varying on the fast scale, which satisfy

$$\Delta_y \mathbf{w} = \nabla_y \pi - \mathbf{I}, \quad y \in \Omega_{\mathrm{b}}(\omega), \tag{7}$$

$$\nabla_y \cdot \mathbf{w} = 0, \quad y \in \Omega_{\mathrm{b}}(\omega), \tag{8}$$

$$\mathbf{w} = 0, \quad y \in \partial\Omega, \tag{9}$$

where $\mathbf{I}$ is the second-order identity tensor, and $\mathbf{w}$ and π are extended to all of Ω by taking their values in the ice Ω_{i} to be 0. In these equations, the w_{ij} component of $\mathbf{w}$ is the jth component of the velocity due to a unit pressure gradient in the ith direction, and π_j is the jth component of the associated scaled pressure. By averaging the leading order term of the velocity v_0 over y or realizations ω, denoted by $\langle\cdot\rangle$, one can obtain the macroscopic equations governing the flow through the porous medium,

$$v(x) = -\frac{1}{\mu}\mathbf{k} \cdot \nabla p(x), \tag{10}$$

$$\nabla \cdot v(x) = 0, \tag{11}$$

where $p(x) = p_0(x)$ and

$$\mathbf{k} = \langle \mathbf{w}(y,\omega) \rangle, \tag{12}$$

the effective permeability tensor. Eq. (10) is known as Darcy's law and Eq. (11) is the macroscopic incompressibility condition. These macroscopic equations were obtained by Allaire (1997, 1992) for periodic media through an appropriate limit as $\epsilon \to 0$. We shall be interested in the permeability in the vertical direction $k_{zz} = k$, in units of m^2.

An important approach to analyzing the behavior of fluids in porous media, or any transport phenomenon through a heterogeneous medium for that matter, is network modeling or approximation (Koplik, 1982; Berkowitz and Balberg, 1992; Sahimi, 1995; Dullien, 1992; Torquato, 2002; Wong et al., 1984; Chayes and Chayes, 1986; Golden, 1997). From a practical standpoint, these networks consist of random or regular arrays of pipes. The geometry, connectedness, and sizes of the basic elements in these networks must reflect the characteristics of the porous medium being modeled. In Fig. 1, a numerical simulation of a two-dimensional flow past a bed of discs of two different sizes is displayed. It is easy to see from this image how a network of pipes could provide a reasonable approximation to this flow. One can also see from this image that there are certain portions of the connected pore space which carry an appreciable part of the flow, while there are other portions which do not. As noted by Torquato (2002), estimates of effective permeability based only on simple pore statistics such as porosity are generally ineffective.

Pipe networks are often studied by relating the problem of fluid flowing through them to the problem of electrical current flowing similarly. As mentioned in Section 1, because of the appearance of a length scale in fluid problems which does not arise in similar electrical conductivity problems, the scalings required to obtain infinite volume or homgenization limits are different. For example, consider the d-dimensional bond lattice connecting nearest neighbor points in the integer lattice $\mathbb{Z}^d$. The bonds are assigned electrical conductivities from a probability distribution. The most common and simply defined probabilistic model is to assign the conductivites to be $\sigma_1 \geqslant 0$ with probability p and $\sigma_2 > 0$ with probability $1 - p$, where the assignments are independent from one another. For purposes of the discussion, let us consider a three-dimensional network, and a cubic $L \times L \times L$ sample of the bond lattice. We attach a perfectly conducting plate to
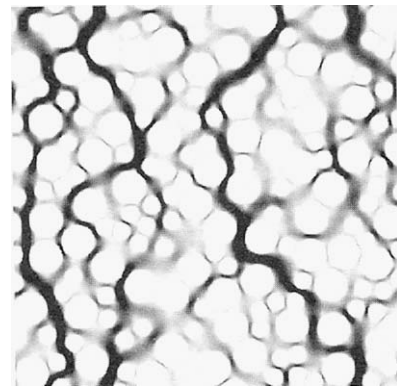

Fig. 1. Simulation of Stokes flow through a bed of disks of two different radii (from Torquato (2002), similar to images of Martys and Garboczi (1992)). In this gray-scale image, black indicates the highest fluid speeds, and white indicates no flow. Note how the velocity field tends to concentrate into channels of least resistance to the flow.

two opposite faces. Let $\Sigma_L(p)$ be the effective conductance of this network, which is the total current that flows through the cube divided by the potential difference maintained between the plates, as determined by Kirchoff's laws. Alternatively, we consider a random pipe network where the bonds are assigned the fluid conductivity $r_1^2/8\mu$, or fluid permeability $r_1^2/8$, with probability p, and the fluid conductivity $r_2^2/8\mu$, with probability $1 - p$. Let $K_L(p)/\mu$ be the effective fluid conductance of this network, which is the rate at which fluid input from one face of the cube flows through an opposing face, given a unit pressure gradient. In the uniform case with $p = 1$, $\Sigma_L(p)$ and $K_L(p)/\mu$ exhibit the following characteristic scalings (Chayes and Chayes, 1986; Golden, 1997):

$$\Sigma_L(p) \sim aL^{d-2}, \quad L \to \infty, \tag{13}$$

$$\frac{K_L(p)}{\mu} \sim \frac{b}{\mu}L^{d-1}, \quad L \to \infty, \tag{14}$$

for constants a and b. For finite volumes these relations are not exact due to boundary effects. Then the effective electrical conductivity $\sigma(p)$ and effective fluid permeability $k(p)$ for the infinite lattice can be obtained through the following scaled limits:

$$\sigma(p) = \lim_{L \to \infty} L^{2-d}\Sigma_L(p), \tag{15}$$

$$k(p) = \lim_{L \to \infty} L^{1-d}K_L(p). \tag{16}$$

The existence of the infinite volume limit and the validity of the ergodic theorem was proven for electrical conductivity and equivalent problems in the continuum for $0 < h < \infty$, with $h = \sigma_1/\sigma_2$ by Kozlov (1978), Papanicolaou and Varadhan (1982), and Golden and Papanicolaou (1983). In the case $h = 0$ or $h = \infty$ a similar result was proven by Zhikov (1989). The nature of the approximation of fluid networks by electrical networks, and the existence of the infinite volume limit for bulk fluid transport coefficients have been addressed by Koplik (1982), Berkowitz and Balberg (1992), Sahimi (1995), Dullien (1992), and other authors.

2.2. Diffusion and trapping in a porous medium

The results of Torquato and Pham (2004) which provide the rigorous basis for our pipe bounds are derived in terms of the trapping constant γ for a porous medium. As discussed in Section 1, knowledge of the trapping constant γ or mean survival time τ is relevant to NMR imaging of the micro-

structure of a porous medium such as sea ice. Furthermore, in view of the principal features of bacterial foraging in a fluid filled porous medium (Vetter et al., 1998), knowledge of these parameters, or closely related quantities, may yield insights into life sustaining processes for sea ice micro-organisms. Through the release of extracellular enzymes (EE) into a fluid filled porous medium and subsequent reactions with particulate organic matter (POM) comprising some part of the solid matrix, microbes can obtain resulting dissolved organic matter (DOM) they need to live (Vetter et al., 1998). We thus formulate the trapping problem in a porous medium, given its close connection to our pipe bounds, as well as its relevance to biological and chemical diffusion processes in the brine microstructure of sea ice. The following formulation of the trapping problem (Torquato, 2002) provides a framework which encompasses some key, albeit simplified features of these important processes.

Consider the problem of a tracer, such as an enzyme or a magnetized hydrogen nucleus, diffusing in the fluid phase $\Omega_b(\omega) \subset \Omega \subset \mathbb{R}^3$ of a porous medium. The tracer reacts with partially or completely absorbing *traps* on the boundary $\partial\Omega_b(\omega)$ of the pore space for each realizatation ω of the random porous medium (Θ, P). The traps comprise the entire surface $\partial\Omega_i(\omega)$ of the ice or some portion of the solid boundary. The traps themselves may represent particulate sediment entrained in the sea ice having nutritive organic content. Let $c(x, y, t, \omega)$, with x and y in Ω_b as above, be the time dependent concentration of the reactant governed by the diffusion equation

$$\frac{\partial c}{\partial t} = D\Delta c + G, \quad x \in \Omega_b(\omega), \tag{17}$$

with the boundary condition on the pore-trap interface,

$$D\frac{\partial c}{\partial n} + \kappa c = 0, \quad x \in \partial\Omega_b(\omega). \tag{18}$$

In (17), D is the diffusion coefficient of the reactant in the fluid filling the pore space, κ is a positive surface reaction rate constant, and G is a generation rate of reactant per unit trap-free volume. In (18), n is the unit outward normal from the pore space. As a particle diffuses in the trap-free region, or the pore space $\Omega_b(\omega)$, it is absorbed on the boundary of the solid matrix with a probability related to the surface rate constant κ. A dimensionless surface rate constant $\kappa^* = \kappa\ell/D$, where ℓ is a characteristic

pore length, can be used to distinguish different regimes of influence:

$$\kappa^* \ll 1 \quad \text{(diffusion-controlled)},$$
$$\kappa^* \gg 1 \quad \text{(reaction-controlled)}.$$

In the diffusion-controlled regime, D is small relative to $\kappa\ell$, and a reactant will typically diffuse in the pore space for much longer than the characteristic time associated with the surface reaction. In the limit of infinite surface reaction $\kappa \to \infty$, the boundary condition on the pore-trap interface becomes a perfectly absorbing *Dirichlet condition*, with $c = 0$ on $\partial\Omega_b(\omega)$ wherever the traps are located. In the reaction-controlled regime, D is large relative to $\kappa\ell$, and a reactant will typically diffuse in the pore space for a relatively short time before if hits a trap and has a chance to react. For vanishing surface reaction rate $\kappa = 0$, the boundary condition on the pore-trap interface becomes a perfectly reflecting *Neumann condition*, with $\frac{\partial c}{\partial n} = 0$.

We now consider the steady state problem in the diffusion-controlled limit of infinite surface reaction $\kappa \to \infty$, with the perfectly absorbing boundary condition $c = 0$ at the pore-trap interfaces (Torquato, 2002). The rate of removal of the reactant by the absorbing boundaries in this case is exactly compensated by the production rate per unit volume G of the reactant. Then the diffusion equation (17), or mass conservation equation, becomes a Poisson equation

$$D\Delta c = -G, \quad x \in \Omega_b(\omega), \quad c = 0, \quad x \in \partial\Omega_b(\omega). \tag{19}$$

Assume again that the parameter $\epsilon = \ell/L$ is small, and that the microstructure Ω_b, as characterized by $\mathscr{I}$, and concentration, or probability density c exhibit dependence upon a slow scale x and a fast scale $y = x/\epsilon$ as discussed above, while $G = G(x)$. Then

$$D\Delta c^\epsilon(x) = -G(x), \quad x \in \Omega_b(\omega),$$
$$c^\epsilon(x) = 0, \quad x \in \partial\Omega_b(\omega). \tag{20}$$

The macroscopic behavior is derived again through a two-scale expansion

$$c^\epsilon(x) = \epsilon^2 c_0(x, y, \omega) + \epsilon^3 c_1(x, y, \omega) + \cdots$$

with the leading order equation $D\Delta_y c_0(x, y, \omega) = -G(x)$, $x \in \Omega_b(\omega)$ and boundary condition $c_0(x, y, \omega) = 0$, $x \in \partial\Omega_b(\omega)$. A scaled concentration field u defined by $c_0(x, y, \omega) = D^{-1}G(x)u(y, \omega)$ solves

$$\Delta_y u(y, \omega) = -1, \quad x \in \Omega_b(\omega),$$
$$u(y, \omega) = 0, \quad x \in \partial\Omega_b(\omega), \tag{21}$$

where $u = 0$ in the region $\Omega_i(\omega)$ and is thus defined throughout Ω. Averaging the defining relation for u yields the macroscopic constitutive relation for the trapping problem,

$$G(x) = \gamma D C(x), \tag{22}$$

where C is an averaged concentration $C(x) = \langle c_0(x, y, \omega) \rangle$ and γ is the *trapping constant*,

$$\gamma^{-1} = \langle u(y, \omega) \rangle = \langle u(y, \omega)\mathscr{I}(y, \omega) \rangle. \tag{23}$$

The trapping constant γ, and its relation to the mean survival time τ, can be understood physically as follows (Torquato, 2002). Let the total number of diffusing Brownian particles created in the pore space per unit time be N and the total number of particles exterior to the traps at a given time be N_0. Then the *average trapping rate* per particle β_{tr} is given by

$$\beta_{tr} = \frac{N}{N_0}.$$

The *mean survival time* τ of a Brownian particle in the pore space is the inverse of the trapping rate,

$$\tau = \beta_{tr}^{-1} = \frac{N_0}{N}. \tag{24}$$

Since $N = G\phi$ and $N_0 = CV$, where $V = |\Omega|$,

$$\tau = \frac{1}{\gamma\phi D} = \frac{\langle u \rangle}{\phi D}. \tag{25}$$

In terms of the survival time τ the macroscopic consitutive law (22) can be written as

$$C(x) = \tau\phi G(x), \tag{26}$$

even though there is no underlying *local* constitutive law. It is useful to note that when the pore space becomes disconnected the trapping constant does not exhibit critical behavior as does the fluid permeability, electrical conductivity, or effective diffusivity near a percolation threshold. Roughly speaking, γ^{-1}, which has units of (length)^2 like the permeability k, is a measure of the average pore size. A Brownian particle in a fluid pore still diffuses for some time before hitting the boundary, whether or not that pore is disconnected from much larger, connected fluid structures. On the other hand, in the absence of any conducting pathways across a sample, the bulk permeability or conductivity of the sample vanishes.

2.3. The trapping problem and relaxation of nuclear magnetization

As mentioned in Section 1, magnetic resonance imaging of sea ice microstructure (Eicken et al., 2000) is a promising avenue for characterizing sea ice as a porous medium and how its microstructure and transport properties evolve with temperature and other parameters. Here we review some results (Torquato, 2002; Torquato and Avellaneda, 1991; Sahimi, 1995) which make precise the connection between the mean survival time considered in the previous subsection, and relaxation processes in nuclear magnetic resonance (NMR) imaging.

In Eq. (17), the time dependent diffusion equation with trap surface boundary condition in Eq. (18), let the source be a Dirac point measure at $t = 0$ with mass c_0, or $G = c_0 \delta(t)$. The solution $c(x, t)$ of Eq. (17) can be expanded in the orthonormal eigenfunctions $\psi_n(x)$ of the Laplacian operator Δ on the pore space $\Omega_b(\omega)$ with boundary conditions (18),

$$c(x, t) = c_0 \sum_{n=1}^{\infty} a_n e^{-t/T_n} \psi_n(x),$$

$$a_n = \frac{1}{V_b} \int_{\Omega_b(\omega)} \psi_n(x) \, dx, \tag{27}$$

where $V_b = |\Omega_b|$,

$$\Delta \psi_n = -\lambda_n \psi_n, \quad x \in \Omega_b(\omega), \tag{28}$$

$$D \frac{\partial \psi_n}{\partial n} + \kappa \psi_n = 0, \quad x \in \partial \Omega_b(\omega). \tag{29}$$

The diffusive relaxation times T_n are related to the spectrum of Δ by

$$T_n = \frac{1}{D \lambda_n}. \tag{30}$$

For long times, the term associated with the smallest eigenvalue λ_1, or the largest or principal relaxation time T_1, dominates the expansion.

The survival probability $S(t)$ is defined in terms of an average of the concentration $c(x, t)$ at time t compared to the initial amount c_0,

$$S(t) = \frac{1}{V_b} \int_{\Omega_b(\omega)} \frac{c(x, t)}{c_0} \, dx, \tag{31}$$

which is the fraction of Brownian particles that survive until time t, with $S(0) = 1$. If the orthonormal expansion (27) is substituted into the integral for $S(t)$, then

$$S(t) = \sum_{n=1}^{\infty} a_n^2 e^{-t/T_n}. \tag{32}$$

In NMR imaging, the protons in the hydrogen atoms of water carry magnetic spin, so that they can align in an external magnetic field. Because the molecules are thermally agitated, not all of them will align with the field. Once the field is turned off, the characteristic time T_1 associated with a return to equilibrium, is called a relaxation time. Experiments show that the relaxation time for a container of water is very different than for water saturating a porous medium (Sahimi, 1995). The relaxation time T_1, as reflected in the spectrum of Δ on $\Omega_b(\omega)$, is strongly affected by surface relaxation mechanisms. It is sensitive to the microstructure of the porous medium and provides insight into the structure of the pore space. Let $m(x, t)$ be the density of the proton magnetization in the z-direction, and m_0 be the initial total magnetization, equivalent to c and c_0 above. Further, let $m(t)$ be the averaged magnetization density. Then, as in (31), the dimensionless, volume averaged magnetization arising in NMR is the survival time,

$$S(t) = \frac{m(t)}{m_0}. \tag{33}$$

Finally, we relate the mean survival time τ considered in the previous subsection to $S(t)$. Torquato and Avellaneda (1991) find the following two expressions:

$$\tau = \sum_{n=1}^{\infty} a_n^2 T_n = \int_0^{\infty} S(t) \, dt \tag{34}$$

and the following inequalities can be then be proved:

$$a_1^2 T_1 \leqslant \tau \leqslant T_1. \tag{35}$$

3. Bounds on the trapping constant and fluid permeability of a porous medium

3.1. Characterizing the microstructure of a porous medium

As discussed in Section 1, the presence of a length scale in fluid problems which does not appear in electrical conductivity and related problems complicates the estimation and bounding of the fluid permeability and trapping constant of a porous medium. In fluid problems in a porous medium this length scale generally appears via the two-point

correlation function. Before defining the two-point function, let us first define the *one-point function* $S_1(x)$ as the probability that a point at position $x \in \Omega$ lies in the brine phase (Torquato, 2002),

$$S_1(x) = P\{\mathscr{I}(x) = 1\} = \langle \mathscr{I}(x) \rangle, \tag{36}$$

which is just the porosity,

$$S_1 = \phi. \tag{37}$$

The *two-point correlation function* $S_2(r)$ is the probability that two points at positions $x \in \Omega$ and $x + r \in \Omega$ both lie in the brine phase,

$$\begin{aligned} S_2(r) &= P\{\mathscr{I}(x) \cdot \mathscr{I}(x + r) = 1\} \\ &= \langle \mathscr{I}(x) \cdot \mathscr{I}(x + r) \rangle. \end{aligned} \tag{38}$$

If the medium is statistically isotropic then $S_2(r)$ depends only on the magnitude $|r|$ of r. The general form of $S_2(r)$ provides information about the gross features of the microstructure of the porous medium. For example, Torquato (2002) considers the two-point functions for two random arrays of spheres. First, an array with possibly overlapping disks is shown, and its two-point function decays monotonically to its asymptotic value ϕ^2 at $|r| = 2a$, where a is the radius of the disks. On the other hand, for an array of *non-overlapping* disks, $S_2(r)$ initially decays towards its asymptotic value as $r \to \infty$ of ϕ^2 near $|r| = 2a$ as well, but exhibits oscillations for small $|r|$ around ϕ^2, indicative of short range order, with a period on the order of the disk diameters $2a$. This behavior reflects spatial correlations between particles due to excluded volume or hard-core effects (Torquato, 2002). It is interesting to note that this oscillatory behavior of the two-point function $S_2(r)$ from horizontal cross-sections, is clearly exhibited for the brine inclusions in sea ice (Perovich and Gow, 1991). Such behavior is consistent with the excluded volume effects displayed by the brine inclusions and their preferred arrangement on the boundaries of the ice platelets. The amplitude of the oscillations in $S_2(r)$ found by Perovich and Gow (1991) increases substantially with temperature.

3.2. Variational formulation of fluid transport in a porous medium

The bounds which we will apply to the fluid permeability and trapping constant in sea ice are derived from energy variational principles. In order to formulate the bounds (Torquato and Pham,

2004; Torquato, 2002), let us first state the energetic definitions for the trapping constant and fluid permeability. In the trapping problem, the scaled concentration field u satisfies Eq. (21), and the trapping constant γ is given by $\gamma^{-1} = \langle u\mathscr{I} \rangle$. Under the ergodicity assumptions discussed above, the trapping constant can be written in terms of the energy functional,

$$\gamma^{-1} = \langle \nabla u(x) \cdot \nabla u(x) \mathscr{I}(x) \rangle. \tag{39}$$

This quadratic form representation for γ^{-1} is obtained from $\Delta u = -1$ by multiplying by u and integrating by parts, where the boundary terms vanish in the infinite volume limit. In the fluid permeability problem, the effective fluid permeability tensor can be expressed as $\mathbf{k} = \langle \mathbf{w} \rangle$, where the Stokes velocity tensor $\mathbf{w}$ is defined in Eqs. (7)–(9). Equivalently, $\mathbf{k}$ can be expressed in terms of the energy functional,

$$\mathbf{k} = \langle \nabla \mathbf{w} : \nabla \mathbf{w} \mathscr{I} \rangle, \tag{40}$$

where the symbol : denotes contraction with respect to two indices (Torquato, 2002). It follows from this representation that the permeability tensor $\mathbf{k}$ is symmetric and positive definite.

For the trapping constant, we are interested in the variational lower bound,

$$\gamma \geqslant \frac{\alpha^2}{\langle \nabla v(x) \cdot \nabla v(x) \mathscr{I}(x) \rangle} \quad \forall v \in \mathscr{T}(\Omega_b), \tag{41}$$

where $\mathscr{T}(\Omega_b)$ is the set of admissible *trial* or *test* concentration fields defined by

$$\mathscr{T}(\Omega_b) = \{\text{ergodic } v(x) \text{ satisfying } \Delta v(x) = -\alpha, x \in \Omega_b\}. \tag{42}$$

For fluid permeability in the isotropic case with $\mathbf{k} = k\mathbf{I}$, the corresponding variational upper bound on k is given by

$$k \leqslant \frac{\langle \nabla \mathbf{q} : \nabla \mathbf{q} \mathscr{I}(x) \rangle}{\beta^2} \quad \forall \mathbf{q} \in \mathscr{T}^*(\Omega_b), \tag{43}$$

where $\mathscr{T}^*(\Omega_b)$ is the set of admissible *trial* or *test* velocity vector fields defined by

$$\begin{aligned} \mathscr{T}^*(\Omega_b) = \{&\text{ergodic } \mathbf{q}(x) \text{ satisfying } \nabla \\ &\times (\Delta \mathbf{q} + \beta \mathbf{e}) = 0, \ x \in \Omega_b\}, \end{aligned} \tag{44}$$

for a unit vector $\mathbf{e}$. The variational inequality (43) generalizes to a statement about positive definite, second-order tensors in the anisotropic case.

It is somewhat surprising that, as we will see below, effective properties characterizing diffusion in a porous medium, such as γ, are closely related

to effective properties characterizing bulk transport from flow, such as k. There is a general inequality relating these two types of problems (Torquato, 2002). For any ergodic porous medium, possibly anisotropic, with $\mathbf{k}$, γ, τ, and D defined above,

$$\mathbf{k} \leqslant \gamma^{-1}\mathbf{I} = D\phi\tau\mathbf{I}. \tag{45}$$

Equivalently, $(\gamma^{-1}\mathbf{I} - \mathbf{k})$ is a positive definite, symmetric, second-order tensor.

3.3. Void bounds on fluid transport properties of porous media

A void trial field $v(x)$ was constructed for the trapping problem in three dimensions by Torquato and Rubinstein (1989). The generalization of this field to any dimension $d \geqslant 2$ (Torquato, 2002) is given by

$$v(x) = \frac{1}{\phi_S} \int_\Omega g(x - y)[\mathscr{I}(y) - \phi]\,dy, \tag{46}$$

where $\phi_S = 1 - \phi$ is the solid ice volume fraction, and $g(x,y)$ is the free space Green's function for the Laplacian Δ. With $r = |x - y|$,

$$g(r) = \begin{cases} -\frac{1}{2\pi}\ln r, & d = 2, \\ \frac{1}{(d-2)\Omega(d)}r^{2-d}, & d \geqslant 3, \end{cases} \tag{47}$$

where $\Omega(d) = 2\pi^{d/2}/\Gamma(d/2)$ is the total solid angle contained in a d-dimensional sphere, and $\Gamma(z)$ is the Gamma function. Substitution of the trial field $v(x)$ in (46) into the variational lower bound (41) on γ with $\alpha = 1$ yields the two-point *void lower bound* for trapping,

$$\gamma \geqslant \frac{\phi_S^2}{\ell_P^2}, \tag{48}$$

where ℓ_P is a pore length scale defined by

$$\ell_P^2 = -\int_0^\infty (S_2(r) - \phi^2)r\ln r\,dr, \quad d = 2, \tag{49}$$

$$\ell_P^2 = \frac{1}{d-2}\int_0^\infty (S_2(r) - \phi^2)r\,dr, \quad d \geqslant 3. \tag{50}$$

For fluid permeability, a void trial tensor field $\mathbf{q}(x)$ similar to the test field $v(x)$ above, inserted into the variational upper bound (43), yields the two-point *void upper bound* for permeability in three and higher dimensions,

$$k \leqslant \frac{(d+1)(d-2)}{d^2 - 3}\frac{\ell_P^2}{\phi_S^2}, \quad d \geqslant 3. \tag{51}$$

The void bounds encompassed by the inequalities (48) and (51) hold for all ergodic microstructures sharing the same porosity ϕ and pore length scale ℓ_P (Torquato and Pham, 2004).

4. Pipe bounds for permeability and trapping in sea ice

4.1. Void bounds on fluid transport for coated spheres and cylinders

For effective conductivity and bulk modulus of statistically isotropic two phase composites, the bounds of Hashin and Shtrikman (1962) are the best possible. They incorporate information from the two-point correlation function. However, when the medium is isotropic, the relevant integrals involving $S_2(r)$ depend only on the volume fractions and dimension of the system, and not on any length scale inherent in $S_2(r)$. The Hashin–Shtrikman bounds are optimal given the volume fractions, in that they are *realizable* by certain composite geometries (Hashin and Shtrikman, 1962; Milton, 2002; Torquato, 2002), including arrays of coated spheres in three dimensions and coated cylinders in two-dimensional systems (Hashin and Shtrikman, 1962). For fluid transport, various bounds on the fluid permeability k and trapping constant γ have been found and used extensively (Torquato, 2002; Sahimi, 1995). However, prior to the results of Torquato and Pham (2004), microstructures which exactly realize any of these bounds in the literature had yet to be identified. As pointed out in Section 1, the main obstacle in such problems is the dependence of the transport coefficients like γ and k on a length scale which does not arise in the conductivity and elasticity problems. These effective parameters depend nontrivially on the two-point and higher order correlation functions in a way that is fundamentally different than for conductivity and elasticity. The void bounds of the previous section depend explicitly on the two-point function $S_2(r)$ and have been evaluated for various particle models (Torquato, 2002; Sahimi, 1995; Milton, 2002).

The composite microgeometries (Hashin and Shtrikman, 1962; Torquato and Pham, 2004) which attain the Hashin–Shtrikman bounds consist of arrays of coated spheres in $d = 3$ or coated cylinders in $d = 2$. In $d = 3$, the composite spheres are composed of a spherical core of phase 1 (inclusion) with radius R_I, surrounded by a concentric shell of phase 2 (matrix) of radius R_M. The ratio $(R_I/R_M)^3$ is fixed

and equal to the inclusion volume fraction ϕ, and these composite spheres fill all space. While there are restrictions on the distribution of the sphere radii in order to fill all space, without loss of generality one can assume that there is a discrete, infinite set of radii corresponding to the sphere sizes in the model. Let ρ_k be the number density of the kth type of composite sphere of outer radius R_{M_k} with corresponding inclusion radius R_{I_k}. The nth moment of the distribution of R_I can be written as

$$\langle R_I^n \rangle = \frac{1}{\rho} \sum_{k=1}^{\infty} \rho_k R_{I_k}^n, \tag{52}$$

where ρ is a normalization constant and $n \geqslant 3$. In $d = 2$ the spheres are replaced by cylindrical cores of phase 1 (inclusion) with radius R_I, surrounded by a concentric cylindrical shell of phase 2 (matrix) of radius R_M. The ratio $(R_I/R_M)^2$ is fixed and equal to the inclusion volume fraction ϕ, and these composite cylinders fill all space.

Torquato and Pham (2004) explicitly evaluate the void bounds on k and γ for the coated sphere and coated cylinder geometries. In some cases the void bounds are *optimal*, since the exact solutions for k and γ in these cases coincide with the expressions for k and γ appearing in the bounds. The void lower bound on the trapping constant in $d = 3$ is realized by coated sphere geometries—not just with the Hashin–Shtrikman size distribution, but with any reasonable size distribution for nonoverlapping spheres. This optimal, two-point void lower bound is given by

$$\gamma \geqslant \frac{15\langle R_I^3 \rangle}{\phi \langle R_I^5 \rangle}. \tag{53}$$

In terms of the mean survival time τ in (34), the lower bound on γ in (53) yields a general upper bound on τ for geometries with spherical inclusions in $d = 3$,

$$\tau = \frac{1}{\gamma \phi D} \leqslant \frac{1}{15D} \frac{\langle R_I^5 \rangle}{\langle R_I^3 \rangle}. \tag{54}$$

The void bounds can be explicitly calculated as well for coated cylinder geometries in $d = 2$. The lower void bound on the trapping constant,

$$\gamma \geqslant \frac{8\langle R_I^2 \rangle}{\phi \langle R_I^4 \rangle}, \tag{55}$$

is again optimal, being attained by the exact result for the coated cylinder model. For the corresponding survival time,

$$\tau \leqslant \frac{1}{8D} \frac{\langle R_I^4 \rangle}{\langle R_I^2 \rangle}. \tag{56}$$

Now think of the inner cylinders as pipes coated by the solid matrix, and consider fluid flow inside bundles of parallel, circular cylindrical tubes, corresponding to the coated cylinder model. The velocity field has only an axial component, and the Stokes equations reduce to the same Poisson equation arising in the trapping problem, as observed by Torquato (1990, 2002). These observations, discussed further below, lead to the exact result in the case of parallel tubes that

$$k = \gamma^{-1}. \tag{57}$$

Thus, for axial flow inside parallel cylindrical tubes occupying a volume fraction ϕ,

$$k \leqslant \frac{\phi \langle R_I^4 \rangle}{8\langle R_I^2 \rangle}. \tag{58}$$

This bound is again optimal, and is attained by the exact result for the coated cylinder model.

It is useful here to calculate explicitly the permeability and trapping constant for a parallel array of cylinders, all of the same radius. We will use this model for sea ice microstructure, and see directly as well how this simple geometry attains the $d = 2$ void bounds. Consider the steady state flow of a viscous fluid through a cylindrical tube with circular cross-section of radius a (Torquato, 2002). Since the brine channels in sea ice have a preferred vertical orientation, let us assume the tube has as its axis the vertical or x_3-axis in $\mathbb{R}^3$. Assuming the no-slip boundary condition on the inner surface of the tube, the Stokes equations reduce to

$$\frac{1}{r} \frac{\partial}{\partial r} \left(r \frac{\partial w}{\partial r} \right) = -1, \quad r < a, \tag{59}$$

$$w = 0, \quad r = a, \qquad w < \infty, \quad r = 0, \tag{60}$$

where $w(r)$ represents the radial dependence of the vertical component of the scaled velocity field. The right side of (59) is the constant, scaled pressure gradient. The solution of (59) and (60) is

$$w(r) = \frac{1}{4}(a^2 - r^2), \quad 0 \leqslant r \leqslant a. \tag{61}$$

The permeability of one cylindrical pipe of radius a is the average of w over the disk of radius a centered at the origin,

$$k = \frac{1}{\pi a^2} \int_0^{2\pi} \int_0^a w(r) r \, dr \, d\theta = \frac{a^2}{8}. \tag{62}$$

Consider now an infinite set of parallel pipes each of inner radius a uniformly distributed throughout an impermeable solid to form a porous medium, such that the volume fraction of the fluid phase contained in the tubes is ϕ. Then the effective permeability k of this porous medium is

$$k = \frac{\phi a^2}{8}. \tag{63}$$

For this medium of porosity ϕ and fixed inclusion radius, the ratio of moments $\langle R_I^4 \rangle / \langle R_I^2 \rangle$ is just a^2. Thus, the parallel pipe porous medium is a model which attains the optimal bound (58). As noted above (Torquato, 1990, 2002) for circular cylindrical tubes, the Stokes equation (59) for the velocity is equivalent to the Poisson equation for the concentration in the trapping problem. Thus, for this parallel pipe porous medium, we have as well for the trapping constant and mean survival time,

$$\frac{1}{\gamma} = \frac{\phi a^2}{8} \quad \text{and} \quad \tau = \frac{a^2}{8D}. \tag{64}$$

4.2. Comparison of void bounds with sea ice permeability data

The brine microstructure in sea ice exhibits strong anisotropy, with the brine inclusions tending to be highly elongated in the vertical direction. Furthermore, especially during warming, these inclusions tend to coalesce and form channels or pipes through the ice matrix, with strongly preferred vertical orientation (Weeks and Ackley, 1986; Eicken, 2003). In Fig. 2, some of these brine channels from Arctic sea ice are displayed, and in Fig. 4, we show some large brine pipes in Antarctic sea ice, as viewed from the surface of the ice, under sunny conditions with temperatures around 0 °C. Several studies, such as those by Eicken et al. (2000), Perovich and Gow (1996), and Bock and Eicken (2005), have provided extensive statistics of the cross-sectional areas A and morphologies of oriented brine inclusions in sea ice. The measurements are taken over a wide range of temperatures and brine volumes ϕ. Given the generally cylindrical shape of an inclusion with cross-sectional area $A \approx \pi R^2$, where R is the cylinder radius, measurements of the average area $\langle A \rangle$ yield an estimate of the average pipe radius $\langle R \rangle$, or pore length scale entering into the fluid transport bounds. As an optimal microgeometry whose permeability exactly coincides with the void upper bound on k in (58), we use the parallel tube model with porosity ϕ and pipe radii $a = \langle R \rangle$. The permeability of the parallel pipe model, $k = \phi a^2 / 8$ in (63), provides a
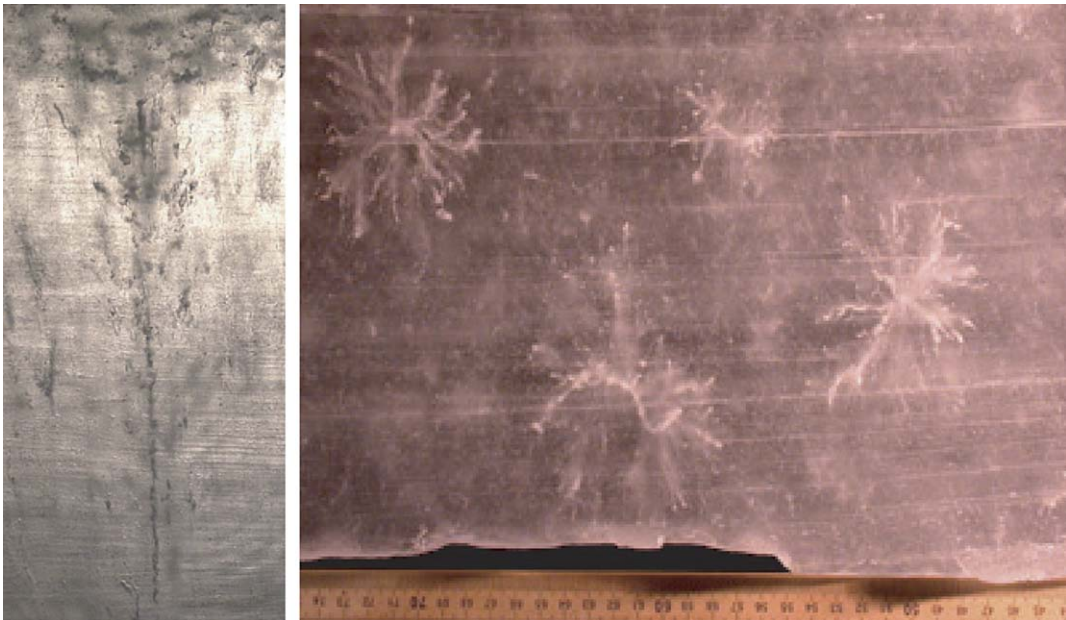

Fig. 2. Vertical (left) and horizontal (right) section photographs of brine channels in Chukchi Sea landfast first-year sea ice sampled near Barrow, Alaska on March 30, 2004. The image on the left corresponds to 15–40 cm depth in the ice column. The image on the right shows part (20 cm × 30 cm) of a horizontal section, obtained from serial sections (photographs by J. Miner, based on refinement of an approach developed by Cole and Shapiro (1998)).

theoretical upper bound for the vertical permeability of sea ice.

Perovich and Gow (1996) and Bock and Eicken (2005) find that the average cross-sectional area $\langle A \rangle$ increases substantially with temperature or brine volume fraction ϕ. To incorporate this important effect, keeping in mind that we seek an *upper bound* on k, we note that the variable data on $\langle A \rangle$ range from about 0.015 mm^2 for ϕ near 0, to about 0.035 mm^2 near $\phi = 0.25$. As a simple model to estimate the observed data on $\langle A \rangle$ obtained by Perovich and Gow (1996), we allow the radius $a = \langle R \rangle$ to increase linearly from $a = 7 \times 10^{-5}$ m (or $a = 0.07$ mm) when $\phi \approx 0$ to $a = 11 \times 10^{-5}$ m (or $a = 0.1$ mm) at $\phi = 0.25$. Thus, our *pipe bound* for the vertical fluid permeability k of sea ice is

$$k \leqslant \frac{\phi [a(\phi)]^2}{8}, \quad a(\phi) = 7 \times 10^{-5} + (1.6 \times 10^{-4})\phi. \tag{65}$$

It has been observed by Perovich and Gow (1996) that the cross-sectional areas A of the brine inclusions can be described by a lognormal distribution with probability density function

$$f(A) = \frac{1}{\sqrt{2\pi\beta^2}} \frac{1}{A} \exp\left[\frac{-(\ln A - \alpha)^2}{2\beta^2}\right], \tag{66}$$

where α and β are the mean and standard deviation of $\ln A$. More information about k can be obtained from further analysis of this distribution function

(Zhu et al., submitted for publication; Heaton et al., 2005). We note that via Eq. (57), our upper pipe bound on the permeability yields a lower bound on the trapping constant, $\gamma \geqslant 8/\phi[a(\phi)]^2$.

In Fig. 3, we compare our pipe bound (65) with laboratory data on k taken on sea ice grown in an indoor tank. Given that the curve is a theoretical upper bound on the values of k, it compares well with the data. The data shown in Fig. 3 were taken by Freitag (1999) and Eicken within the framework of the multidisciplinary Large Scale Facility experiment INTERICE 1996/1997. The ice was grown in the 30-m-long Arctic Environmental Test Basin of the Hamburg Ship Model Basin in Hamburg, Germany. The indoor tank was 6 m wide and 1 m deep. During a freezing cycle of 8 days ice formation was induced by air temperatures down to −16 °C, which resulted in approximately 15–20 cm of new ice. Afterwards, during a 7 day warming period the formerly negative temperature gradient within the ice is changed to a slightly positive one. The bulk salinity decreases to values of 2–3 ppt. Before the permeability is measured the ice samples are centrifuged at the sampling site at the in situ temperature, using a method developed by Weissenberger et al. (1992). The separation of the brine preserves the original pore space even when the samples are stored and handled at colder temperatures. The samples have a cylindrical form with approximately 9 cm in diameter and 6 cm in length. In the laboratory experiments, a fluid of known viscosity is pressed through an ice sample, applying a constant imposed
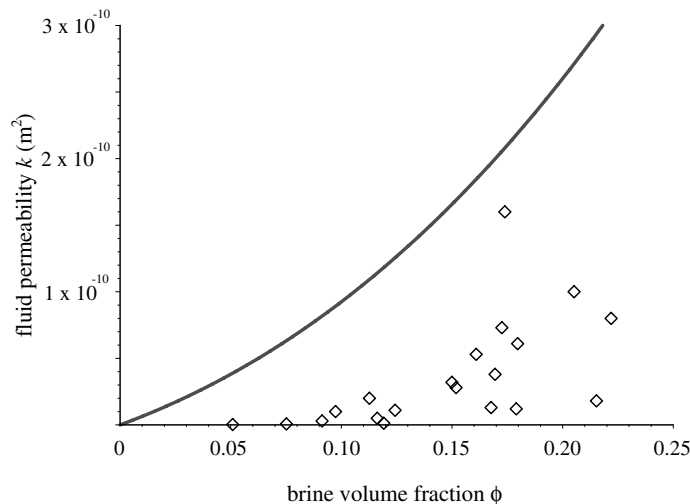

Fig. 3. The void upper bound in (65) is represented by the curve above. It captures laboratory data on the vertical fluid permeability of artificially grown sea ice.

driving force. By measuring the specific discharge, and the pressure drop along the sample, the permeability can be calculated from Darcy's law. The fluid used for the measurements is N-decane ($C_{10}H_{22}$). N-decane is insoluble in water and therefore has little effect on the sea ice matrix. Its melting point is $-30\,°C$ with density and viscosity values approximately 20% lower than brine values.

During a measurement cycle, the mean of 5–20 permeability values at different pressure levels is found. Imposed pressures do not exceed 70 mbar. The induced flow direction through the ice matrix corresponds to the vertical direction through sea ice in situ. The main uncertainty in the method arises from the centrifuging process. An incomplete release of brine as well as temperature variations between the sampling and centrifuging time could have significant influence. In our measurements it is assumed that the error caused by temperature variations are negligible because of only slight temperature gradients during summer. But freezing of retained brine leads to underestimations. With an assumption of a uniform reduction of radii in a simplified pore model of vertical tubes, the permeability would be underestimated by a factor of 0.6 if the maximal amount of 20% of retained brine (Weissenberger et al., 1992) is expected. However errors in pressure, outflow measurements and data processing do not exceed 10%, so that in sum a possible uncertainty in the permeability values comes to about 50%. The experimental set up is suitable for permeability measurements between 10^{-16} and $10^{-7}\,m^2$. The upper limit is given by the restriction of Darcy's law to laminar flow. The lower range for permeability estimation is limited by the increasing amount of time required to measure such small flows, to many hours and longer.

During the Mertz Glacier Polynya Experiment, 16 July–7 September 1999, aboard RSV *Aurora Australis*, Golden and Lytle conducted measurements of percolation processes in first year sea ice in the vicinity of 144 °E and 66 °S. As mentioned above, flooding of a snow layer on the surface of sea ice through upward brine percolation, and subsequent freezing of the slush, is an important mechanism for ice production in some regions of the Antarctic. This process is also essential for supplying nutrients to algal communities growing in the ice. To assess the level of ice production or nutrient replenishment through brine percolation processes, it would be useful to be able to obtain an overall upper bound on the vertical fluid permeability of

the sea ice, which incorporates information about the large channels present in warmed sea ice, which are not considered in the averages reported by Perovich and Gow (1996). During a particularly warm period around 12–15 August, where air temperatures got as high as about 0 °C, and the ice surface temperatures were in the -4 to $-5\,°C$ range, we cleared away the snow and observed extensive arrays of brine tubes at the sea ice surface, which extended at least some centimeters into the ice, presumably much further. The ice was less than 50 cm thick. We constructed three *percolation pits*, or square meter areas with the snow cleared off, during two of the ice stations. We estimated the number of well developed brine tubes, measured their diameters, measured temperatures, and took photos and video of these structures. A photo of these large brine pipes from the surface of the ice, and a photo of the percolation pit are displayed in Fig. 4. The estimates for the number of tubes with about 1 cm diameters were 60–65, 90–100, and 100–120 per m^2. Interestingly, in the second pit over about a 15 min period after the snow was cleared away we observed that about 2 cm of brine had flooded the surface of the ice in one corner of the pit. We encountered warm, thin, brine soaked, porous sea ice during that period, with large numbers of open channels. It is reasonable to assume that we encountered sea ice under conditions where the porosity and vertical permeability were near the upper end of possible values. As an approximate, global upper bound on the vertical permeability of sea ice, we evaluate the parallel pipe model using the following parameters: about 100 pipes per square meter, with total porosity $\phi = 0.01$, each pipe has a diameter of 1 cm, or radius $a = 5 \times 10^{-3}\,m$. Then using the pipe medium expression (63) for k, and assuming that these large pipes carry the bulk of the fluid being transported, yields a general upper bound of

$$k \leqslant 3 \times 10^{-8}\,m^2. \tag{67}$$

This constant plays a central role in further analysis of the permeability of sea ice, and arises from a completely different analysis of the sea ice microstructure used in continuum percolation theory (Heaton et al., 2005). This constant also lies above, just slightly in some cases, all the data and numerical simulations of sea ice permeability of Freitag (1999). It should be remarked, though, that an additional factor (>1) may be necessary in this global bound to incorporate information on variations in pipe sizes, which are not considered here.

Fig. 4. On the left is a photo (taken by Golden) of the surface of warm, porous sea ice in Antarctica, showing large brine channels. On the right is a photo (taken by A. Roberts) showing a percolation pit with the *Aurora Australis* and Golden in the background.

References

Ackley, S.F., Lytle, V.I., Golden, K.M., Darling, M.N., Kuehn, G.A., 1995. Sea ice measurements during ANZFLUX. Antarctic J. U. S. 30, 133–135.

Allaire, G., 1992. Homogenization and two-scale convergence. SIAM J. Math. Anal. 23, 261–298.

Allaire, G., 1997. One-phase Newtonian flow. In: Hornung, U. (Ed.), Homogenization and Porous Media. Springer-Verlag, pp. 45–68.

Berkowitz, B., Balberg, I., 1992. Percolation approach to the problem of hydraulic conductivity in porous media. Transport Porous Media 9, 275–286.

Berryman, J.G., Milton, G.W., 1985. Normalization constraint for variational bounds on fluid permeability. J. Chem. Phys. 83, 754–760.

Bock, C., Eicken, H., 2005. A magnetic resonance study of temperature-dependent microstructural evolution and self-diffusion of water in Arctic first-year sea ice. Ann. Glaciol. 40, in press.

Carmack, E.C., 1986. Circulation and mixing in ice-covered waters. In: Untersteiner, N. (Ed.), The Geophysics of Sea Ice. Plenum Press, pp. 641–712.

Chayes, J.T., Chayes, L., 1986. Bulk transport properties and exponent inequalities for random resistor and flow networks. Comm. Math. Phys. 105, 133–152.

Cole, D.M., Shapiro, L.H., 1998. Observations of brine drainage networks and microstructure of first-year sea ice. J. Geophys. Res. 103 (C10), 21739–21750.

Cox, G.F.N., Weeks, W.F., 1975. Brine drainage and initial salt entrapment in sodium chloride ice. Research Report 354, USA CRREL, Hanover, NH.

DeBondt, S., Froyen, L., Deruyttere, A., 1992. Electrical conductivity of composites: a percolation approach. J. Mater. Sci. 27, 1983–1988.

Dullien, F.A.L., 1992. Porous Media, Fluid Transport and Pore Structure, second ed. Academic Press, New York.

Eicken, H., 1992. The role of sea ice in structuring Antarctic ecosystems. Polar Biol. 12, 3–13.

Eicken, H., 2003. Growth, microstructure and properties of sea ice. In: Thomas, D.N., Dieckmann, G.S. (Eds.), Sea Ice: An Introduction to its Physics, Chemistry, Biology and Geology. Blackwell, Oxford, pp. 22–81.

Eicken, H., Bock, C., Wittig, R., Miller, H., Poertner, H.-O., 2000. Nuclear magnetic resonance imaging of sea ice pore fluids: Methods and thermal evolution of pore microstructure. Cold Reg. Sci. Technol. 31, 207–225.

Freitag, J., 1999. The hydraulic properties of Arctic sea ice - Implications for the small-scale particle transport. Ber. Polarforsch. 325, 150 (in German).

Fritsen, C.H., Lytle, V.I., Ackley, S.F., Sullivan, C.W., 1994. Autumn bloom of Antarctic pack-ice algae. Science 266, 782–784.

Golden, K.M., 1997. Percolation models for porous media. In: Hornung, U. (Ed.), Homogenization and Porous Media. Springer-Verlag, pp. 27–43.

Golden, K., Papanicolaou, G., 1983. Bounds for effective parameters of heterogeneous media by analytic continuation. Comm. Math. Phys. 90, 473–491.

Golden, K.M., Ackley, S.F., Lytle, V.I., 1998a. The percolation phase transition in sea ice. Science 282, 2238–2241.

Golden, K.M., Borup, D., Cheney, M., Cherkaeva, E., Dawson, M.S., Ding, K.H., Fung, A.K., Isaacson, D., Johnson, S.A., Jordan, A.K., Kong, J.A., Kwok, R., Nghiem, S.V., Onstott, R.G., Sylvester, J., Winebrenner, D.P., Zabel, I., 1998b. Inverse electromagnetic scattering models for sea ice. IEEE Trans. Geosci. Rem. Sens. 36 (5), 1675–1704.

Golden, K.M., Cheney, M., Ding, K.H., Fung, A.K., Grenfell, T.C., Isaacson, D., Kong, J.A., Nghiem, S.V., Sylvester, J., Winebrenner, D.P., 1998c. Forward electromagnetic scattering models for sea ice. IEEE Trans. Geosci. Rem. Sens. 36 (5), 1655–1674.

Hashin, Z., Shtrikman, S., 1962. A variational approach to the theory of effective magnetic permeability of multiphase materials. J. Appl. Phys. 33, 3125–3131.

Heaton, A.L., Eicken, H., Golden, K.M., 2005. Theory and measurements of fluid permeability in sea ice. Preprint.

Hornung, U. (Ed.), 1997. Homogenization and Porous Media. Springer, New York.

Hosseinmostafa, A.R., Lytle, V.I., Jezek, K.C., Gogineni, S.P., Ackley, S.F., Moore, R.K., 1995. Comparison of radar backscatter from Antarctic and Arctic sea ice. J. Electromagnetic Appl. 9, 421–438.

Janzen, J., 1975. On the critical conductive filler loading in antistatic composites. J. Appl. Phys. 46 (2), 966–969.

Janzen, J., 1980. Short derivation of the influence of particle size ratio on the conductivity threshold in binary aggregates. J. Appl. Phys. 51 (4), 2279–2280.

Jeffries, M.O. (Ed.), 1998. Antarctic Sea Ice: Physical processes, interactions and variability. American Geophysical Union, Washington, DC.

Kattenberg, A., Giorgi, F., Grassl, H., Meehl, G.A., Mitchell, J.F.B., Stouffer, R.J., Tokioka, T., Weaver, A.J., Wigley, T.M.L., 1996. Climate models—projections of future climate. In: Houghton, J.T., Filho, L.G.M., Callander, B.A., Harris, N., Kattenberg, A., Maskell, K. (Eds.), Climate Change 1995. The Science of Climate Change. Cambridge University Press, Cambridge, pp. 285–357.

Keller, J.B., 1980. Darcy's law for flow in porous media and the two-space method. In: Sternberg, R.L. (Ed.), Nonlinear Partial Differential Equations in Engineering and Applied Sciences. Dekker, pp. 429–443.

Koplik, J., 1982. Creeping flow in two-dimensional networks. J. Fluid Mech. 119, 219–247.

Kozlov, S.M., 1978. Averaging random structures (in Russian). Dokl. Akad. Nauk SSSR 241, 1016.

Kusy, R.P., 1977. Influence of particle size ratio on the continuity of aggregates. J. Appl. Phys. 48 (12), 5301–5303.

Kusy, R.P., Turner, D.T., 1971. Electrical resistivity of a polymeric insulator containing segregated metallic particles. Nature 229, 58.

Lizotte, M.P., Arrigo, K.R. (Eds.), 1998. Antarctic Sea Ice: Biological Processes, Interactions and Variability. American Geophysical Union, Washington, DC.

Lytle, V.I., Ackley, S.F., 1996. Heat flux through sea ice in the Western Weddell Sea: Convective and conductive transfer processes. J. Geophys. Res. 101 (C4), 8853–8868.

Lytle, V.I., Golden, K.M., 1995. Microwave backscatter measurements from first year pack ice in the eastern Weddell Sea. Antarctic J. U. S. 30, 125–127.

Maksym, T., Jeffries, M.O., 2001. Phase and compositional evolution of the flooded layer during snow-ice formation of Antarctic sea ice. Ann. Glaciol. 33, 37–44.

Malliaris, A., Turner, D.T., 1971. Influence of particle size on the electrical resistivity of compacted mixtures of polymeric and metallic powders. J. Appl. Phys. 42 (2), 614–618.

Martys, N., Garboczi, E.J., 1992. Length scales relating the fluid permeability and electrical conductivity in random two-dimensional model porous media. Phys. Rev. B 46, 6080–6090.

Milton, G.W., 2002. Theory of Composites. Cambridge University Press, Cambridge.

Ono, N., Kasai, T., 1985. Surface layer salinity of young sea ice. Ann. Glaciol. 6, 298–299.

Papanicolaou, G., Varadhan, S., 1982. Boundary value problems with rapidly oscillating coefficients. In: Colloquia Mathematica Societatis János Bolyai 27, Random Fields (Esztergom, Hungary 1979). North-Holland, p. 835.

Perovich, D.K., Gow, A.J., 1991. A statistical description of the microstructure of young sea ice. J. Geophys. Res. 96 (C9), 16943.

Perovich, D.K., Gow, A.J., 1996. A quantitative description of sea ice inclusions. J. Geophys. Res. 101 (C8), 18327–18343.

Perovich, D.K., Andreas, E.L., Curry, J.A., Eicken, H., 1999. Year on ice gives climate insights. EOS, Transact. Am. Geophys. Union 80, 485–486.

Prager, S., 1961. Viscous flow through porous media. Phys. Fluids 4, 1477–14822.

Priou, A. (Ed.), 1992. Dielectric Properties of Heterogeneous Materials. Elsevier, New York.

Rubinstein, J., Torquato, S., 1989. Flow in random porous media: Mathematical formulation variational principles, and rigorous bounds. J. Fluid Mech., 206.

Sahimi, M., 1995. Flow and Transport in Porous Media and Fractured Rock. VCH, Weinheim.

Saito, T., Ono, N., 1978. Percolation of sea ice. I. Measurements of kerosene permeability of NaCl ice. Low Temp. Sci. A37, 55–62.

Serreze, M.C., Walsh III., J.E.F.S.C., Osterkamp, T., Dyurgerov, M., Romanovsky, V., Oechel, W.C., Morison, J., Zhang, T., Barry, R.G., 2000. Observational evidence of recent change in the northern high-latitude environment. Climatic Change 46, 159–207.

Stauffer, D., Aharony, A., 1992. Introduction to Percolation Theory, second ed. Taylor and Francis Ltd., London.

Sturm, M., Perovich, D.K., Serreze, M.C., 2003. Meltdown in the North. Scientific American, October.

Tartar, L., 1980. Incompressible fluid flow in a porous medium. In: Sanchez-Palencia, E. (Ed.), Non-Homogeneous Media and Vibration Theory, Lecture Notes in Physics, vol. 129. Springer-Verlag, pp. 368–377.

Thomas, D.N., Dieckmann, G.S., 2002. Antarctic sea ice—a habitat for extremophiles. Science 295, 641–644.

Thomas, D.N., Dieckmann, G.S. (Eds.), 2003. Sea Ice: An Introduction to its Physics, Chemistry, Biology and Geology. Blackwell, Oxford.

Torquato, S., 1990. Relationship between permeability and diffusion-controlled trapping constant of porous media. Phys. Rev. Lett. 64, 2644–2646.

Torquato, S., 2002. Random Heterogeneous Materials: Microstructure and Macroscopic Properties. Springer-Verlag, New York.

Torquato, S., Avellaneda, M., 1991. Diffusion and reaction in heterogeneous media: Pore size distribution, relaxation times, and mean survival time. J. Chem. Phys. 95, 6477–6489.

Torquato, S., Pham, D.C., 2004. Optimal bounds on the trapping constant and permeability of porous media. Phys. Rev. Lett. 92, 255505:1–4.

Torquato, S., Rubinstein, J., 1989. Diffusion-controlled reactions. II. Further bounds on the rate constant. J. Chem. Phys. 90, 1644–1647.

Trodahl, H.J., McGuiness, M.J., Langhorne, P.J., Collins, K., Pantoja, A.E., Smith, I.J., Haskell, T.G., 2000. Heat transport in McMurdo Sound first-year fast ice. J. Geophys. Res. 105 (C5), 11347–11358.

Untersteiner, N. (Ed.), 1986. The Geophysics of Sea Ice. Plenum, New York.

Untersteiner, N., 1990. Structure and dynamics of the Arctic Ocean ice cover. In: Grant, A., Johnson, L., Sweeney, J.F. (Eds.), The Arctic Ocean Region. Geological Society of America, Boulder, Colorado.

Vetter, Y.A., Deming, J.W., Jumars, P.A., Krieger-Brockett, B.B., 1998. A predictive model of bacterial foraging by means of freely released extracellular enzymes. Microb. Ecol. 36, 75–92.

Weeks, W.F., Ackley, S.F., 1986. The growth, structure and properties of sea ice. In: Untersteiner, N. (Ed.), The Geophysics of Sea Ice. Plenum Press, New York, pp. 9–164.

Weissenberger, J., Dieckmann, G., Gradinger, R., Spindler, M., 1992. Sea ice: a cast technique to examine and analyze brine pockets and channel structure. Limnol. Oceanogr. 37, 179–183.

Wong, P., Koplick, J., Tomanic, J.P., 1984. Conductivity and permeability of rocks. Phys. Rev. B 30, 6606–6614.

Zhikov, V.V., 1989. Effective conductivity of random homogeneous sets. Math. Zametki 45, 34.

Zhu, J., Jabini, A., Golden, K.M., Eicken, H., Morris, M., submitted for publication. A network model for fluid transport in sea ice. Ann. Glaciol.